Published in final edited form as:
Circ Res. 2010 October 1; 107(7): 851–859. doi:10.1161/CIRCRESAHA.109.215269.

Cardiac small conductance Ca^{2+}-activated K^+ (SK) channel subunits form heteromultimers *via* the coiled-coil domains in the C-termini of the channels

Dipika Tuteja[1], **Sassan Rafizadeh**[1], **Valeriy Timofeyev**[1], **Shuyun Wang**[1], **Zheng Zhang**[1], **Ning Li**[1], **Robertino K Mateo**[1], **Anil Singapuri**[1], **J. Nilas Young**[2], **Anne A. Knowlton**[1,3], and **Nipavan Chiamvimonvat**[1,3]

[1]Division of Cardiovascular Medicine, University of California, Davis

[2]Division of Cardiothoracic Surgery, University of California, Davis

[3]Department of Veterans Affairs, Northern California Health Care System, Mather, CA

Abstract

Summary—Small conductance Ca^{2+}-activated K^+ (SK) channels have recently been documented in human and mouse cardiac myocytes that contribute importantly towards cardiac action potential profiles. Three isoforms of SK channel subunits (SK1, 2 and 3) have been demonstrated in the heart. The channels are more prominently expressed in atrial and pacemaking tissues compared to the ventricles. Significance of the channels is underscored by the findings that SK2 channels may play a role in atrial fibrillation. The present study demonstrates the heteromultimerization of different SK channel subunits in human and mouse atrial myocytes. Moreover, the study provides evidence for the direct interaction between the coiled-coil domains in the C-termini of the different SK subunits. Disruption of the coiled-coil domain interaction results in a significant decrease in the Ca^{2+}-activated K^+ current in atrial myocytes which is important for cardiac repolarization. Formation of heteromeric channels provides an increase in functional diversity for K^+ channels. Moreover, different isoforms of SK channels may represent therapeutic targets to directly modify atrial cells without interfering with ventricular myocytes. Thus, new knowledge into the structure and function of SK channels is important not only from a fundamental viewpoint, but might also have important therapeutic implications in cardiac arrhythmias.

Rationale—Ca^{2+}-activated K^+ channels are present in a wide variety of cells. We have previously reported the presence of small conductance Ca^{2+}-activated K^+ (SK or K_{Ca}) channels in human and mouse cardiac myocytes that contribute functionally towards the shape and duration of cardiac action potentials. Three isoforms of SK channel subunits (SK1, 2 and 3) are found to be expressed. Moreover, there is differential expression with more abundant SK channels in the atria and pacemaking tissues compared to the ventricles. SK channels are proposed to be assembled as tetramers similar to other K^+ channels, but the molecular determinants driving their subunit interaction and assembly are not defined in cardiac tissues.

Nipavan Chiamvimonvat, Division of Cardiovascular Medicine, Department of Medicine, University of California, Davis, One Shields Avenue, GBSF 6315, Davis, CA 95616, voice: (530) 754-7158, fax: (530) 754-7167: nchiamvimonvat@ucdavis.edu.

Disclosures: None.

Objective—The goal of the study is to investigate the heteromultimeric formation and the domain necessary for the assembly of three SK channel subunits (SK1-3) into complexes in human and mouse hearts.

Methods and Results—Here, we provide evidence to support the formation of heteromultimeric complexes among different SK channel subunits in native cardiac tissues. SK1, 2 and 3 subunits contain coiled-coil domains (CCDs) in the C-termini. *In vitro* interaction assay supports the direct interaction between CCDs of the channel subunits. Moreover, specific inhibitory peptides derived from CCDs block the Ca^{2+}-activated K^+ current in atrial myocytes which is important for cardiac repolarization.

Conclusions—The data provide evidence for the formation of heteromultimeric complexes among different SK channel subunits in atrial myocytes. Since SK channels are predominantly expressed in atrial myocytes, specific ligands of the different isoforms of SK channel subunits may offer a unique therapeutic opportunity to directly modify atrial cells without interfering with ventricular myocytes.

Keywords

Ca^{2+}-activated K^+ channels; cardiac myocytes; heteromultimerization; coiled-coil domains

Introduction

Small conductance Ca^{2+}-activated K^+ (SK or $K_{Ca}2$) channels belong to a family of Ca^{2+}-activated K^+ channels (K_{Ca}), which have been reported from a wide variety of cells.[1,2] K_{Ca} channels represent a highly unique family of K^+ channels in that they are directly gated by changes in intracellular Ca^{2+} concentration and hence, function to integrate changes in Ca^{2+} concentration with changes in K^+ conductance and membrane potentials. K_{Ca} channels have been extensively studied in central and peripheral nervous system where they mediate afterhyperpolarizations (AHPs) following action potentials (AP);[1,3] however, their functional importance in cardiac tissues is only beginning to be elucidated.[4-11] Indeed, evidence for the existence of SK channels in the heart were first established by our laboratory[4,5] and has since been supported by work from others.[6,8] We have identified several isoforms of SK channel subunits in the heart including SK1, SK2 and SK3 ($K_{Ca}2.1$, 2.2 and 2.3) and have documented that SK channels are highly expressed and play important functional roles in atrial myocytes and pacemaking tissues compared to the ventricle.[4,5,7,9,10] Genetic ablation of SK channels in a mouse model results in atrial AP prolongation and atrial arrhythmias.[10] Overexpression of SK2 channels in a transgenic mouse model results in the shortening of the spontaneous APs of the atrioventricular node cells and an increase in the firing frequency. On the other hand, ablation of the SK2 channel results in the opposite effects.[9]

SK channels are being increasingly recognized as possible drug targets in diseases such as myotonic muscular dystrophy and sickle cell anemia.[12,13] SK channels are encoded by three genes, *KCNN1*, *KCNN2*, *KCNN3*, and exhibit characteristic sensitivity to bee venom peptide toxin, apamin, with potency of blocking dependent on the specific isoforms.[1,2,14] Conceptually, SK channels specificity could be accomplished by homomeric as well as heteromeric assembly.[15,16] Indeed, heteromeric co-assembly of SK channel subunits has been demonstrated in heterologous expression systems.[14-18] However, structural determinants of SK channel assembly in heteromeric as well as homomeric complexes remain unknown. Here, we provide evidence to support the formation of heteromeric complexes among different SK channel subunits in native cardiac tissues. A combination of molecular, biochemical, and electrophysiological techniques were used to directly determine the structural determinants of the heteromeric complexes. Sequence analyses of SK channel

proteins suggest the occurrence of coiled-coil domains (CCD) in the C-termini of these channels. Moreover, we have provided data to support the roles of CCD in mediating SK channel subunit interaction and assembly using *in vitro* interaction assay as well as functional analyses.

Materials and Methods

The human study protocol was approved by Institutional Review Board. All animal care and procedures were approved by Institutional Animal Care and Use Committee. Detailed methods are presented in Online Data Supplement.

Immunofluorescence confocal microscopy and immunogold-labeled transmission electron microscopy (immuno-EM)

Immunofluorescence confocal microscopy and immune-EM were performed as described previously.[4,11]

Co-immunoprecipitation and Western blot analysis

Human heart tissues were procured from a commercial source (T Cubed, Inc.). Co-immunoprecipitation (co-IP) and Western blot were performed as described previously.[7]

Sequence analysis and design of inhibitory peptides

Coils Version 2.2 program (http://www.ch.embnet.org) was used for the prediction of CCDs from primary amino acid sequence of mouse and human cardiac SK channels.[19-22] The α-helix structure of CCD2 was confirmed by homology modeling of structural coordinates of SK2 amino acid sequence with those of template models from the servers: Swiss-model (http://swissmodel.expasy.org/workspace/index.php?func=modelling_simple1) and I-TASSER (http://zhang.bioinformatics.ku.edu/I-TASSER).[23]

In vitro interaction assays

Mammalian Two-Hybrid System Assay 2 (Clontech, Palo Alto, CA) was used for testing the *in vitro* interactions among SK1, 2 & 3 channel subunits. C-termini fusion constructs of SK1-3 were generated in pM & pVP16 vectors from mouse cardiac SK1 channel (accession # AY258143.1),[5] amino acids 395-580 of human cardiac SK2 channel (accession # AY258141.1)[4] and amino acids 544-737 of human cardiac SK3 channel (accession # AY258142.1; Online Figure I).

Ca^{2+}-activated K^+ current ($I_{K,Ca}$) recordings

Whole-cell $I_{K,Ca}$ was recorded from freshly isolated atrial myocytes and transfected tsA201 cells using patch-clamp techniques as previously described.[4,24]

Results

Subcellular distribution of SK1, SK2, & SK3 channel subunits in isolated mouse atrial myocytes

We have previously documented the existence of SK1, 2 & 3 channel subunits in human and mouse hearts.[4,5] In order to determine the subcellular distribution of SK1, SK2, and SK3 channel subunits in mouse atrial cardiomyocytes, we performed immunofluorescence confocal microscopy using double labeling with anti-SK1, SK2 and SK3 antibodies (Figure 1A, B, C, respectively). There was overlap in the distribution of the three isoforms of SK channel subunits along the Z-lines in atrial myocytes. The degree of overlap in the subcellular distribution was directly quantified using scatter plots as shown in the right

panels demonstrating a high degree of correlation between different SK channel subunits. Merged images are shown at higher magnification in the right panels below the scatter plots. Control experiments were performed as presented in Supplemental Material including 1) Preincubation of anti-SK antibodies with antigenic peptide (AP) (Online Figure IIA), 2) Secondary antibodies only (Online Figure IIB), 3) Staining using homozygous SK2 knockout mice as previously described[9,10] (Online Figure IIC), and 4) Immunostaining using tsA201 cells transfected with SK1, 2 or 3 plasmids (Online Figure IID). In addition, immuno-EM was performed to further resolve the subcellular localization of the SK channel subunits. Electron microscopic post-embedding immunogold labeling demonstrates that SK1, SK2 and SK3 channel subunits are clustered together in mouse atrial myocytes (Figure 1D-E).

Identification of heteromultimeric complexes of SK1, SK2, & SK3 channel subunits in human and mouse myocytes using co-immunoprecipitation (co-IP)

To directly determine whether SK1, SK2 and SK3 channel proteins form heteromultimeric complexes in human (Figure 2A-C) and mouse (Figure 2D-F) cardiac tissues, co-IP was performed. Using anti-SK1 antibody, we immunoprecipitated SK1, SK2 and SK3 channel proteins from tissue lysate (Figure 2A-F, Lane 1 & 2). For SK1 channel protein, both monomers and dimers were detected as two distinct bands. Similarly, in the reverse experiments using anti-SK2 antibody (Fig. 2A-F, Lane 3 & 4), and anti-SK3 antibody (Figure 2A-F, Lane 5&6), SK1, SK2, & SK3 channel proteins could be immunoprecipitated from tissue lysate. Specificity of the SK antibodies used was directly tested by pre-incubating the anti-SK antibodies with their corresponding antigenic peptides before immunoblotting the immunoprecipitated complexes from mouse atrial and ventricular tissue (Figure 2G). Control co-IP experiments were also performed by using the normal rabbit-IgG or serum to immunoprecipitate complexes from mouse atrial and ventricular tissues (Figure 2H). The 50 kDa bands correspond to immunoglobulin heavy chain (rabbit host) used in the IP reactions when blotted by anti-SK antibodies generated in the same host. Our previous data have shown that atrial tissues express higher level of the SK subunits, however, the IP in Figure 2 was performed with limited antibody, hence, does not depict quantitative IP. Additional control IP experiments were performed using homozygous SK2 knockout mice (Online Figure IIIA&B).

Sequence analysis of SK channel subunits revealed existence of coil-coiled domains in the C-termini of the channels

To establish the structural determinants mediating the protein-protein interactions, we analyzed amino acid sequences of SK channel subunits using coiled-coil prediction programs (Coils Version 2.2). Figure 3A shows probabilities of coiled-coil formation, which peaked in the C-termini and were very low in the N-termini (except for SK3 channel). The probability of forming coiled-coils of first CCD (CCD1) from C-termini of all three SK channel isoforms was lower than that for the second CCD (CCD2). The coiled-coil probability of CCD1 of SK2 was almost double of that of SK1 & SK3 and was close to the value of the N-terminal CCD of SK3 channel.

Coiled-coils in SK channels followed a continuous stretch of seven-residue sequence repeat (with positions named a-g) containing small hydrophobic residues in the “a” (first) and “d” (fourth) positions. The larger polar residues often occurred at positions “e” and “g” (Figure 3 B). As shown in the Figure, highlighted hydrophobic residues (e.g. Valine (V), Leucine (L), Isoleucine (I)) at “a” and “d” positions would form the hydrophobic core for the interaction, while charged residues at “g” and succeeding “e” positions would establish complementary electrostatic interactions (Figure 3B and Online Figure IIIC). The alignment of bipartite CCDs of SK channels with CCD domains of two other human K^+ channels viz., K_V7 and

K_v10 is presented in Figure 3B for comparison. Figure IIIC in Online Data Supplement depicts the α-helical structure of two CCD2 from two SK2 channel subunits (Pymol software).

Identification of interaction between different SK channel subunits using *in vitro* interaction assay

To further document protein-protein interaction among SK channel subunits, mammalian two-hybrid system was used. The C-terminal fusion constructs of cardiac SK1, SK2 and SK3 channel subunits harboring the CCDs were subcloned into pM vector containing DNA binding domain (BD) and pVP16 vector containing transcription activation domain (AD). C-termini of the SK1-SK3 protein immediately before the start of calmodulin binding domain (CaMBD) as depicted in Figure 4A were used. The SK1-3 c-termini in pM and pVP16 vectors were co-transfected along with secreted alkaline phosphatase vector (pSEAP, containing SEAP reporter gene under the control of a GAL4 responsive element) into tsA201 cells (Online Figure IIID). Alkaline phosphatase activity showed positive interactions between C-termini of SK1, SK2 and SK3 with intensity that was significantly higher (*p<0.05) than negative controls (pM+pVP16 empty vectors, pM-SK1/2/3+pVP16 empty vectors or pM empty vector+pVP16-SK1/2/3). pM3pVP16+pM3pVP16 were used as the positive control (Figure 4B). The strength of interaction observed between SK1 and SK2, SK2 and SK3, & SK1 and SK3 channel subunits were similar. This pattern was also observed when the two different SK channel subunits were reversed in the BD & AD vector, indicating that interactions were not vector specific (Figure 4B). These results support the observed heteromultimeric complexes of SK channel subunits from the co-IP experiments. Finally, deletion of CCD2 domains from the SK2 C termini (SK2-ΔCCD) resulted in a significant decrease in the interaction of the SK2 C termini with SK1 or SK3 C termini (*p<0.05) supporting the importance of CCDs in the heteromultimerization of the SK channel subunits (Figure 4B).

Triple mutations GYG to AAA in SK1 and SK3 channel subunits suppressed wild-type SK2 currents

In our previously published study, we have shown that triple mutations of the pore signature sequence, glycine, tyrosine and glycine (GYG) to alanine (AAA) in SK2 channel subunit renders the mutant subunit non conductive.[10] Moreover, upon co-expression of the mutant subunit with wild-type (WT) SK2 channel subunit, the mutant subunit leads to dominant-negative (DN) suppression of $I_{K,Ca}$. Since SK channel subunits have conserved pore sequence, “GYG”, we set out to mutate pore signature sequence of SK1 as well as SK3 channel subunits by site-directed mutagenesis (GYG to AAA). We tested the DN effect of pore mutants of SK1-AAA and SK3-AAA on WT SK2 currents in transfected tsA201 cells. All transfections were performed in the presence of α-actinin2 based on our previous published data showing an increased SK2 channel expression upon co-transfection with α-actinin2 proteins.[7] We first documented that the three SK pore mutant constructs (SK1/2/3-AAA) could indeed lead to a DN functional knockdown of their WT counterparts in tsA201 cells (Data shown for WT SK2 & AAA-SK2 only). Next, we tested whether the three SK mutant subunits can result in the DN suppression of WT SK2 current (Online Figure IVB-E). Online Figure IVB shows $I_{K,Ca}$ recorded from tsA201 cells transfected with α-actinin2 and SK2 channel. $I_{K,Ca}$ was significantly suppressed by co-expressing WT SK2 with SK2-AAA, showing DN effect of the SK2 pore mutant subunit (Online Figure IVE). Similar suppression of the $I_{K,Ca}$ was observed using SK1 or SK3 pore mutant subunits (Online Figure IVC, D). Summary data are shown in Online Figure IVF. Similar data were obtained showing DN suppression of WT SK3 current (Online Figure V).

SK1, SK2 and SK3 CCD peptides inhibit $I_{K,Ca}$ in atrial myocytes

To further test the roles of CCD in the multi-subunit assembly of SK channels in native cells, we designed a SK2-specific peptide directly targeting the CCD2 region of SK2 channel subunit with the amino acid sequence as underlined in Figure 3B. Inhibition of expressed and endogenous $I_{K,Ca}$ by SK2-specific peptide (inhibitory peptide) was tested in tsA201 cell lines (Figure 5B) and isolated mouse atrial myocytes (Figure 5D), respectively. $I_{K,Ca}$ was recorded using whole-cell patch-clamp techniques one minute after establishment of whole-cell configuration (initial) and after 12 minutes. Inclusion of 30-50 μM inhibitory peptide in the pipette solution resulted in nearly complete inhibition of $I_{K,Ca}$ after 12 minutes of recordings compared to the initial traces (Figure 5B&D) with no further reduction after application of apamin (100 pM). In contrast, parallel experiments using the same concentrations of scrambled peptide (Figure 5A&C) showed stable current recordings at 12 minutes after the establishment of whole-cell configuration with no “run down” or “run up” of $I_{K,Ca}$. Apamin (100 pM) was applied to further document the presence of $I_{K,Ca}$. In addition, SK1- and SK3-specific peptides directly targeting the CCD region of SK1 and SK3 subunits with the amino acid sequence as shown in Fig. 3B were generated. The SK1 and SK3 inhibitory peptides also resulted in the inhibition of $I_{K,Ca}$ recorded from isolated atrial myocytes (Figure 5E&F). However, the effects were less pronounced as compared to the SK2 inhibitory peptide likely due to the lower expression of SK1 and SK3 subunits in atrial myocytes.[7] Summary data in Figure 5G&H shows significant inhibition of the apamin-sensitive $I_{K,Ca}$ quantified at the test potentials of -120 and +60 mV.

We further documented the specificity of the inhibitory peptide. The SK2 inhibitory peptide failed to suppress the SK3 current expressed in tsA 201 cells (Online Figure VIA). In contrast, the peptide resulted in nearly complete inhibition of $I_{K,Ca}$ current from SK2 homomultimers (Figure 5B) or heteromultimers from SK2 and SK3 channel subunits (Online Figure VIB).

Discussion

In the present study, we provide evidence for the formation of heteromultimerization of SK subunits in human and mouse myocytes. We further establish that there is a direct physical interaction of the C-terminal regions among the three SK channel subunits *via* the CCDs. *Finally, we took advantage of specific inhibitory peptides derived from CCDs to demonstrate the inhibition of $I_{K,Ca}$ in atrial myocytes. Taken together the findings using inhibitory peptides as well as in vitro interaction assay with deletion constructs implicate the role of the CCDs as mediators of the heteromeric assembly.*

Heteromultimeric complex formation among SK channel subunits

Ion channel diversity is achieved by several mechanisms ranging from physical association of α subunits with accessory β subunits that modulate channel activities, to alternative splicing and mRNA editing, thus favoring functional ion channel diversity from limited gene products.[25] Moreover, in K^+ channels where the conductive pore is formed by four subunits, functional diversity can be further attained by coassembly of different subunits to generate heteromeric channels with novel biophysical properties.

Coassembly of K^+ channels is precisely controlled by multiple mechanisms, e.g. spatial and temporal co-expression, to prevent wasteful or potentially deleterious combinations from hampering normal cellular functioning.[26] Typically, assembly of K^+ channels into functional homo- and heterotetramers occurs by interaction of tetramerization domains in the N and/or C termini and are conserved within the gene family.[27] Many K^+ channels form heteromultimers *via* the C-terminal regions which resemble tetramerizing-coiled coil (TCC)

domains.[27] TCC domains are continuous stretch of CCDs and have been implicated in the enhancement of tetramer stability and selectivity of multimerization among many K^+ channels.[27,28]

Coiled-coils are bundles of intertwined α-helices constituting structural motif repetitions $(abcdefg)_n$ which are directly involved in protein-protein interactions.[29] CCD serves as sites for dynamic assembly and disassembly of protein complexes in diverse protein classes including transcription factors, fibrous proteins, membrane fusion proteins and motor proteins.[30] Since many coiled-coil bearing proteins play crucial roles in different physiological and pathological processes in addition to the high specificity and reversible nature of the CCD associations, CCDs may represent attractive targets for pharmacological intervention.[31,32] Several studies have suggested the key roles of cytoplasmic CCDs in ion channel assembly including those from members of voltage-gated ion channels superfamily e.g. transient receptor potential ion channels (TRPM),[33] K_V7,[28] and cyclic nucleotide-gated channels.[34]

Although functional heteromeric interaction of SK channels has been documented in heterologous systems,[14-18] it is not clear if these are present in native tissues. Our study provided evidence for the physical coexistence and heteromeric associations among SK channel subtypes in native cardiac cells. In addition, our *in vitro* interaction assays suggested almost similar strengths of interactions among SK channel subtypes. Our results from co-expression of full-length SK2 and DN pore mutants of SK channel subunits further demonstrate the suppression of SK2 current *via* heteromeric interaction by coassembly of different SK DN constructs with WT SK2 subunits. Theoretically, the probability of tetrameric WT channel being formed when equal ratio of DN & WT channel are present is close to 6% ($(1/2)^4$). This is validated by our observation that DN mutant channels resulted in marked suppression of the WT subunits supporting the notion that the presence of even a minimum of one DN monomeric subunit resulted in non-functional channels. These results provide evidence for the ability of SK channel subunits in forming heteromultimers in addition to the formation of homomultimers as deduced from current recorded from SK1, SK2 or SK3 channel subunits when expressed alone.

Functional significance of SK channel heteromultimerization

In cardiac myocytes, SK channels contribute to the late phase of cardiac repolarization whereas in neurons these channels underlie after-hyperpolarization.[4,5] New insights into SK channel subtype heteromeric associations are physiologically significant and relevant since SK channel variants (SK2-sh,[35] SK3-1B,[36] SK3-1C[37]) have previously been documented to produce non-functional channels as homomers in mammalian cells, and can selectively suppress the endogenous SK currents. Other studies have reported existence of truncated isoforms of SK3 channel which trap full-length ion channel proteins intracellularly *via* DN inhibition of functional channel expression on cell surface.[38] Similarly, our previous studies have documented several different splice variants of SK1 and SK3 channels from human and mouse hearts;[5] their functional significance especially in the context of their roles in subunit interactions remain unclear.

Molecular determinants of subunit assembly

Initial reports of SK channel subunit assembly indicate the involvement of the N-terminus.[15,16] Here, our study provides new evidence for additional important molecular determinant involving the CCDs within the C-termini of the channels. More than one domain from SK channel C-terminus has been shown to be responsible for inter-subunit interaction and trafficking. These include the CaMBD distal to S6 transmembrane domain, responsible for Ca^{2+}-independent binding of calmodulin (CaM).[39] Our data provide direct

evidence for the functional roles of CCDs in SK channel subtypes in forming heteromultimeric complexes. Taken together, it appears that more than one region of the channel are involved in SK channel assembly.

Importance of CCD in other K^+ channels

C-terminal CCDs of some K^+ channels ($K_v11.1$, K_v) have been shown to not only drive tetrameric assembly but also determine stability and selectivity of multimerization.[27,28] It is the compatibility of CCDs that determines the heteromeric associations among channel subunits encoded by different genes.[27] Absence of CCD significantly impairs functional channel expression.[40] This is indicative of prominent roles of CCDs primarily in driving K^+ channel subunit assembly. Prevalence of mutations in CCDs of ion channels involved in channelopathies further signifies their important roles. Bipartite CCD domains have been reported from C-termini of K_v7 channels which are known to form hetero-oligomers and play an important role in neuronal excitability.[41] In this study, we demonstrated that similar to K_v7 family, all SK channel subtypes exhibit bipartite C-terminal CCDs (CCD1 & 2) especially for SK2 channel with CCD1 (25 aa) and CCD2 (34 aa). However, the presence of coiled-coil characteristics of only CCD2 of SK2 channels has been confirmed with crystal structure.[42] The bipartite nature of the C-terminus of SK2 channel remains only speculative at this point in time.

Future studies are required to understand the roles of SK channel subunits heteromultimerization while maintaining homomeric SK channel populations in different tissues. In addition, the relative contribution and properties of homomeric and heteromeric channels in the heart remain to be elucidated. Taken together, results from our studies set an important starting point towards monitoring self-assembly, co-assembly and stoichiometry of SK channels in native tissues to dissect roles and significance of SK channels under normal and pathogenic conditions.

Online Figure I. Cloning and sequence of human atrial SK3 (haSK3) used in the study. (A) Representative agarose gel of RT-PCR amplified products from total RNA isolated from two different human atrial samples (Lanes 2 and 3) using primers designed from published human myometrium SK3 (hmSK3, Accession no. AY049734). Lanes 4 & 5 represent RT-PCR amplification of cDNA from the two different samples of human atria using human GAPDH primers. Lane 6 is a negative control (PCR amplified without RT). Lanes 1 and 7 are Hi-Lo ladders (Bionexus). (B) Amino acid sequence alignment (ClustalW) of deduced SK3 protein sequence from human atrium compared to human myometrium SK3. Six predicted transmembrane domains (S1-S6) and pore (P) are highlighted in yellow. Highlighted red stretch in P region represents K^+ selective filter GYG. If, Isoform; ha, human atrium; hmm, human myometrium; CaMBD, calmodulin binding domain in the C terminus. Numbers on right represent length of predicted protein in terms of amino acid residues, while on the left roman numerals denote isoform nomenclature. Dashes represent Gaps in the sequence alignment.

Online Figure II. Confocal photomicrographs of single isolated mouse atrial myocytes doubly stained with (A) anti-SK1, 2 or 3 antibodies pre-incubated with the corresponding antigenic peptides (AP) in different combinations as follows: (Upper Panels) goat anti-SK1 and rabbit anti-SK2, (Middle Panels) rabbit anti-SK2 and mouse anti-SK3, and (Lower Panels) rabbit anti-SK1 and mouse anti-SK3 antibodies. Immunofluorescence labeling was performed by treatment with fluorphore labeled secondary antibodies as in Figure 1. Scale bars are 10 μm. Merged images are shown on the right of each panel. (B) Additional control experiments using secondary antibodies only in different combinations are as follows: (Upper Panels) donkey anti-goat Alexa Fluor 555 and chicken anti-rabbit Alexa Fluor 488, (Middle Panels) donkey anti-mouse Alexa Fluor 555 and chicken anti-rabbit Alexa Fluor

488, and (Lower Panels) chicken anti-rabbit Alexa Fluor 555 and donkey anti-mouse Alexa 488. Scale bars are 10 μm. Merged images are shown in the third column of each panel. Fourth column of each panel shows phase contrast images of the cardiomyoctyes. (C) Representative confocal photomicrographs of single isolated mouse atrial myocytes stained with anti-SK2 antibody as follows: (Upper Panel) from wild-type (WT) mice, (Middle Panel) from wild-type mice but the antibody was pre-treated with antigenic peptide and (Lower Panel) from homozygous SK2 knockout (SK2 KO) mice. Scale bars are 10 μm. (D) tsA201 cells were co-transfected with pIRES-EGFP-SK1, 2 or 3 expression vectors plus pcDNA3-α-actinin2 plasmid labeled as SK1, 2 or 3, respectively. Lack of cross-reactivity between different anti-SK antibodies were demonstrated using immunofluorscence confocal microscopy and anti-SK specific primary antibodies and the corresponding Alexa fluor-labeled secondary antibodies as in Fig 1. Middle panels are DAPI stain for nuclei followed by merged images. The right most panels show the staining at higher magnification. Scale bars are 10 μm.

Online Figure III. Cardiac tissue homogenates from homozygous SK2 knockout mice were immunoprecipitated (IP) with anti-SK1, SK2 or SK3 antibodies. Proteins were eluted and Western blot analysis (IB) was performed using anti-SK1 antibody in (A) and anti-SK3 antibody in (B). Anti-SK2 antibody failed to immunoprecipitate SK1 channel protein in (A) or SK3 channel protein in (B). Negative control was performed by immunoblotting of eluted proteins immunoprecipitated with non-specific IgG (Lane 4 in A and B). (C) Representation of coiled-coil interaction/assembly domain model from two subunits of SK channels. “a” and “d” coiled-coil positions are indicated and color coded as blue and red, respectively. (D) tsA201 cells were transfected with pM-SK1 (SK1-BD), pM-SK2 (SK2-BD), pVP16-SK2 (SK2-AD), pM-SK3 (SK3-BD), pVP16-SK2 (SK2-AD). Cell lysates were used for Western blot (IB) with anti-GAL4 DNA-BD, anti-SK2, and anti-SK3 antibodies.

Online Figure IV. Dominant-negative (DN) suppression of SK2 current by SK1-DN, SK2-DN or SK3-DN constructs in tsA201 cells. Whole-cell apamin-sensitive $I_{K,Ca}$ was elicited using a voltage-ramp protocol from +40 to -100 mV with a slope of -180 V/s from a holding potential of -55 mV in tsA201 cells. $I_{K,Ca}$ density was obtained by normalizing the current to the cell capacitance. (A) non-transfected cells, (B) cells transfected with pIRES2-EGFP-SK2 plasmid encoding full-length human SK2 channel plus pcDNA3-α-actinin2 plasmid, (C,D,E) cells transfected with pIRES2-EGFP-SK2 and pcDNA3-α-actinin2 plasmids plus SK1-DN, SK2-DN or SK3-DN constructs, respectively. (F) Summary data of $I_{K,Ca}$ density at the test potentials of -120 and +60 mV illustrating DN effects on $I_{K,Ca}$ from SK1-DN, SK2-DN or SK3-DN constructs (*$p<0.05$, n = 6-12 cells for each group).

Online Figure V. Dominant-negative (DN) suppression of SK3 current by SK1-DN, SK2-DN or SK3-DN constructs in tsA201 cells. Whole-cell $I_{K,Ca}$ was elicited using a voltage-ramp protocol from +40 to -100 mV with a slope of -180 V/s from a holding potential of -55 mV in tsA201 cells. $I_{K,Ca}$ density was obtained by normalizing the current to the cell capacitance. (A) cells transfected with pIRES2-EGFP-SK3 plasmid encoding full-length human SK3 channel plus pcDNA3-α-actinin2 plasmid, (B,C,D) cells transfected with pIRES2-EGFP-SK3 and pcDNA3-α-actinin2 plasmids plus SK3-DN, SK1-DN or SK2-DN constructs, respectively.

Online Figure VI. (A, B) Peptide derived from the SK2 CCD inhibits whole-cell $I_{K,Ca}$ in tsA201 cells co-expressing SK2 and SK3 subunits but not SK3 subunit alone. (A) Whole-cell $I_{K,Ca}$ was recorded from tsA201 cells co-transfected with pIRES2-EGFP-SK3 and pcDNA3-α-actinin2 plasmids. A voltage-ramp protocol was applied from -120 to +60 mV at a holding potential of -55 mV. $I_{K,Ca}$ current was recorded immediately after establishment of whole-cell mode (black line), 12 minutes thereafter (blue line). (B) Similar experiments

were performed in from tsA201 cells co-transfected with pIRES2-EGFP-SK2, pIRES2-EGFP-SK3 and pcDNA3-α-actinin2 plasmids. Inclusion of 50 μM inhibitory peptide in the pipette solution resulted in nearly complete inhibition of $I_{K,Ca}$ after 12 minutes of recordings compared to the initial traces in cells transfected with both SK2 and SK3 subunits. In contrast, parallel experiments using the same concentrations of inhibitory peptide in cells transfected with SK3 alone showed stable current recordings at 12 minutes after the establishment of whole-cell configuration with no "run down" or "run up" of $I_{K,Ca}$. Similar data were obtained in a total of 6 cells. Experiments were performed in a blinded fashion in which the experimentators had no knowledge of the compositions of the channels expressed.

Supplementary Material

Refer to Web version on PubMed Central for supplementary material.

Acknowledgments

The authors are in debt to Dr. E.N. Yamoah for helpful suggestions and comments.

Sources of Funding: Supported by NIH/NHLBI (RO1 HL075274 and HL085844 to NC) and the VA Merit Review Grant (NC).

References

1. Kohler M, Hirschberg B, Bond CT, Kinzie JM, Marrion NV, Maylie J, Adelman JP. Small-conductance, calcium-activated potassium channels from mammalian brain. Science. 1996; 273:1709–1714. [PubMed: 8781233]
2. Stocker M. Ca^{2+}-activated K^+ channels: molecular determinants and function of the SK family. Nat Rev Neurosci. 2004; 5:758–770. [PubMed: 15378036]
3. Pedarzani P, McCutcheon JE, Rogge G, Jensen BS, Christophersen P, Hougaard C, Strobaek D, Stocker M. Specific enhancement of SK channel activity selectively potentiates the afterhyperpolarizing current I_{AHP} and modulates the firing properties of hippocampal pyramidal neurons. J Biol Chem. 2005; 280:41404–41411. [PubMed: 16239218]
4. Xu Y, Tuteja D, Zhang Z, Xu D, Zhang Y, Rodriguez J, Nie L, Tuxson HR, Young JN, Glatter KA, Vazquez AE, Yamoah EN, Chiamvimonvat N. Molecular identification and functional roles of a Ca^{2+}-activated K^+ channel in human and mouse hearts. J Biol Chem. 2003; 278:49085–49094. [PubMed: 13679367]
5. Tuteja D, Xu D, Timofeyev V, Lu L, Sharma D, Zhang Z, Xu Y, Nie L, Vazquez AE, Young JN, Glatter KA, Chiamvimonvat N. Differential expression of small-conductance Ca^{2+}-activated K^+ channels SK1, SK2, and SK3 in mouse atrial and ventricular myocytes. Am J Physiol Heart Circ Physiol. 2005; 289:H2714–2723. [PubMed: 16055520]
6. Marionneau C, Couette B, Liu J, Li H, Mangoni ME, Nargeot J, Lei M, Escande D, Demolombe S. Specific pattern of ionic channel gene expression associated with pacemaker activity in the mouse heart. J Physiol. 2005; 562:223–234. [PubMed: 15498808]
7. Lu L, Zhang Q, Timofeyev V, Zhang Z, Young JN, Shin HS, Knowlton AA, Chiamvimonvat N. Molecular coupling of a Ca^{2+}-activated K^+ channel to L-type Ca^{2+} channels *via* α-actinin2. Circ Res. 2007; 100:112–120. [PubMed: 17110593]
8. Ozgen N, Dun W, Sosunov EA, Anyukhovsky EP, Hirose M, Duffy HS, Boyden PA, Rosen MR. Early electrical remodeling in rabbit pulmonary vein results from trafficking of intracellular SK2 channels to membrane sites. Cardiovasc Res. 2007; 75:758–769. [PubMed: 17588552]
9. Zhang Q, Timofeyev V, Lu L, Li N, Singapuri A, Long MK, Bond CT, Adelman JP, Chiamvimonvat N. Functional roles of a Ca^{2+}-activated K^+ channel in atrioventricular nodes. Circ Res. 2008; 102:465–471. [PubMed: 18096820]
10. Li N, Timofeyev V, Tuteja D, Xu D, Lu L, Zhang Q, Zhang Z, Singapuri A, Albert TR, Rajagopal AV, Bond CT, Periasamy M, Adelman J, Chiamvimonvat N. Ablation of a Ca^{2+}-activated K^+

channel (SK2 channel) results in action potential prolongation in atrial myocytes and atrial fibrillation. J Physiol. 2009; 587:1087–1100. [PubMed: 19139040]

11. Lu L, Timofeyev V, Li N, Rafizadeh S, Singapuri A, Harris TR, Chiamvimonvat N. α-actinin2 cytoskeletal protein is required for the functional membrane localization of a Ca^{2+}-activated K^+ channel (SK2 channel). Proc Natl Acad Sci U S A. 2009; 106:18402–18407. [PubMed: 19815520]
12. Seutin V, Liegeois JF. SK channels are on the move. Br J Pharmacol. 2007; 151:568–570. [PubMed: 17486139]
13. Blank T, Nijholt I, Kye MJ, Spiess J. Small conductance Ca^{2+}-activated K^+ channels as targets of CNS drug development. Curr Drug Targets CNS Neurol Disord. 2004; 3:161–167. [PubMed: 15180477]
14. Ishii TM, Maylie J, Adelman JP. Determinants of apamin and d-tubocurarine block in SK potassium channels. J Biol Chem. 1997; 272:23195–23200. [PubMed: 9287325]
15. Fanger CM, Rauer H, Neben AL, Miller MJ, Wulff H, Rosa JC, Ganellin CR, Chandy KG, Cahalan MD. Calcium-activated potassium channels sustain calcium signaling in T lymphocytes. Selective blockers and manipulated channel expression levels. J Biol Chem. 2001; 276:12249–12256. [PubMed: 11278890]
16. Miller MJ, Rauer H, Tomita H, Gargus JJ, Gutman GA, Cahalan MD, Chandy KG. Nuclear localization and dominant-negative suppression by a mutant $SK_{Ca}3$ N-terminal channel fragment identified in a patient with schizophrenia. J Biol Chem. 2001; 276:27753–27756. [PubMed: 11395478]
17. Benton DC, Monaghan AS, Hosseini R, Bahia PK, Haylett DG, Moss GW. Small conductance Ca^{2+}-activated K^+ channels formed by the expression of rat SK1 and SK2 genes in HEK 293 cells. J Physiol. 2003; 553:13–19. [PubMed: 14555714]
18. Monaghan AS, Benton DC, Bahia PK, Hosseini R, Shah YA, Haylett DG, Moss GW. The SK3 Subunit of Small Conductance Ca^{2+}-activated K^+ Channels Interacts with Both SK1 and SK2 Subunits in a Heterologous Expression System. J Biol Chem. 2004; 279:1003–1009. [PubMed: 14559917]
19. Lupas A, Van Dyke M, Stock J. Predicting coiled coils from protein sequences. Science. 1991; 252:1162–1164. [PubMed: 2031185]
20. Delorenzi M, Speed T. An HMM model for coiled-coil domains and a comparison with PSSM-based predictions. Bioinformatics. 2002; 18:617–625. [PubMed: 12016059]
21. Berger B, Wilson DB, Wolf E, Tonchev T, Milla M, Kim PS. Predicting coiled coils by use of pairwise residue correlations. Proc Natl Acad Sci U S A. 1995; 92:8259–8263. [PubMed: 7667278]
22. Wolf E, Kim PS, Berger B. MultiCoil: a program for predicting two- and three-stranded coiled coils. Protein Sci. 1997; 6:1179–1189. [PubMed: 9194178]
23. Zhang Y. I-TASSER server for protein 3D structure prediction. BMC Bioinformatics. 2008; 9:40. [PubMed: 18215316]
24. Hamill OP, Marty A, Neher E, Sakmann B, Sigworth FJ. Improved patch-clamp techniques for high-resolution current recording from cells and cell-free membrane patches. Pflugers Arch. 1981; 391:85–100. [PubMed: 6270629]
25. Coetzee WA, Amarillo Y, Chiu J, Chow A, Lau D, McCormack T, Moreno H, Nadal MS, Ozaita A, Pountney D, Saganich M, Vega-Saenz de Miera E, Rudy B. Molecular diversity of K^+ channels. Ann N Y Acad Sci. 1999; 868:233–285. [PubMed: 10414301]
26. Sailer CA, Hu H, Kaufmann WA, Trieb M, Schwarzer C, Storm JF, Knaus HG. Regional differences in distribution and functional expression of small-conductance Ca^{2+}-activated K^+ channels in rat brain. J Neurosci. 2002; 22:9698–9707. [PubMed: 12427825]
27. Jenke M, Sanchez A, Monje F, Stuhmer W, Weseloh RM, Pardo LA. C-terminal domains implicated in the functional surface expression of potassium channels. Embo J. 2003; 22:395–403. [PubMed: 12554641]
28. Howard RJ, Clark KA, Holton JM, Minor DL Jr. Structural insight into KCNQ (Kv7) channel assembly and channelopathy. Neuron. 2007; 53:663–675. [PubMed: 17329207]

29. Wiener R, Haitin Y, Shamgar L, Fernandez-Alonso MC, Martos A, Chomsky-Hecht O, Rivas G, Attali B, Hirsch JA. The KCNQ1 (K_V7.1) COOH terminus, a multitiered scaffold for subunit assembly and protein interaction. J Biol Chem. 2008; 283:5815–5830. [PubMed: 18165683]
30. Woolfson DN. The design of coiled-coil structures and assemblies. Adv Protein Chem. 2005; 70:79–112. [PubMed: 15837514]
31. Contegno F, Cioce M, Pelicci PG, Minucci S. Targeting protein inactivation through an oligomerization chain reaction. Proc Natl Acad Sci U S A. 2002; 99:1865–1869. [PubMed: 11842196]
32. Goodwin DA, Meares CF. Advances in pretargeting biotechnology. Biotechnol Adv. 2001; 19:435–450. [PubMed: 14538068]
33. Tsuruda PR, Julius D, Minor DL Jr. Coiled coils direct assembly of a cold-activated TRP channel. Neuron. 2006; 51:201–212. [PubMed: 16846855]
34. Zhong H, Lai J, Yau KW. Selective heteromeric assembly of cyclic nucleotide-gated channels. Proc Natl Acad Sci U S A. 2003; 100:5509–5513. [PubMed: 12700356]
35. Murthy SR, Teodorescu G, Nijholt IM, Dolga AM, Grissmer S, Spiess J, Blank T. Identification and characterization of a novel, shorter isoform of the small conductance Ca^{2+} -activated K^+ channel SK2. J Neurochem. 2008; 106:2312–2321. [PubMed: 18624921]
36. Tomita H, Shakkottai VG, Gutman GA, Sun G, Bunney WE, Cahalan MD, Chandy KG, Gargus JJ. Novel truncated isoform of SK3 potassium channel is a potent dominant-negative regulator of SK currents: implications in schizophrenia. Mol Psychiatry. 2003; 8:524–535. 460. [PubMed: 12808432]
37. Kolski-Andreaco A, Tomita H, Shakkottai VG, Gutman GA, Cahalan MD, Gargus JJ, Chandy KG. SK3-1C, a dominant-negative suppressor of SK_{Ca} and IK_{Ca} channels. J Biol Chem. 2004; 279:6893–6904. [PubMed: 14638680]
38. Tomita H, Shakkottai VG, Gutman GA, Sun G, Bunney WE, Cahalan MD, Chandy KG, Gargus JJ. Naturally occurring dominant-negative SK3 channel isoform. Mol Psychiatry. 2003; 8:766.
39. Lee WS, Ngo-Anh TJ, Bruening-Wright A, Maylie J, Adelman JP. Small conductance Ca^{2+}-activated K^+ channels and calmodulin: cell surface expression and gating. J Biol Chem. 2003; 278:25940–25946. [PubMed: 12734181]
40. Kupershmidt S, Yang T, Chanthaphaychith S, Wang Z, Towbin JA, Roden DM. Defective human Ether-a-go-go-related gene trafficking linked to an endoplasmic reticulum retention signal in the C terminus. J Biol Chem. 2002; 277:27442–27448. [PubMed: 12021266]
41. Schwake M, Athanasiadu D, Beimgraben C, Blanz J, Beck C, Jentsch TJ, Saftig P, Friedrich T. Structural determinants of M-type KCNQ (K_V7) K^+ channel assembly. J Neurosci. 2006; 26:3757–3766. [PubMed: 16597729]
42. Kim JY, Kim MK, Kang GB, Park CS, Eom SH. Crystal structure of the leucine zipper domain of small-conductance Ca^{2+}-activated K^+ (SK_{Ca}) channel from Rattus norvegicus. Proteins. 2008; 70:568–571. [PubMed: 17910055]

Non-standard Abbreviations and Acronyms

AP	Action potential
CCD	Coiled-coil domain
$\boldsymbol{I_{K,Ca}}$	Ca^{2+}-activated K^+ current
Co-IP	Co-immunoprecipitation
CaMBD	Calmodulin binding domain
DN	Dominant-negative
WT	Wild-type

Novelty and Significance

What is Known?

Small conductance Ca^{2+}-activated K^+ (SK) channels represent a highly unique family of K^+ channels since they are gated solely by changes in intracellular Ca^{2+} concentration and consequently function to integrate changes in Ca^{2+} concentration with changes in K^+ conductance and membrane potentials.

Several isoforms of SK channel subunits including SK1, SK2 and SK3 have been documented to express in the heart and play important functional roles in atrial myocytes and pacemaking tissues compared to the ventricle.

What New Information Does This Article Contribute?

The present work provides evidence for the formation of heteromultimers of the three SK channel subunits in human and mouse atrial myocytes.

In vitro interaction assay provides evidence for a direct physical interaction of the C-terminal regions among the three SK channel subunits.

Using functional analyses, the present study demonstrates that disruption of the subunit interaction via the coiled-coil domain in the carboxyl termini of the channel subunits results in a significant inhibition of Ca^{2+}-activated K^+ current in atrial myocytes.

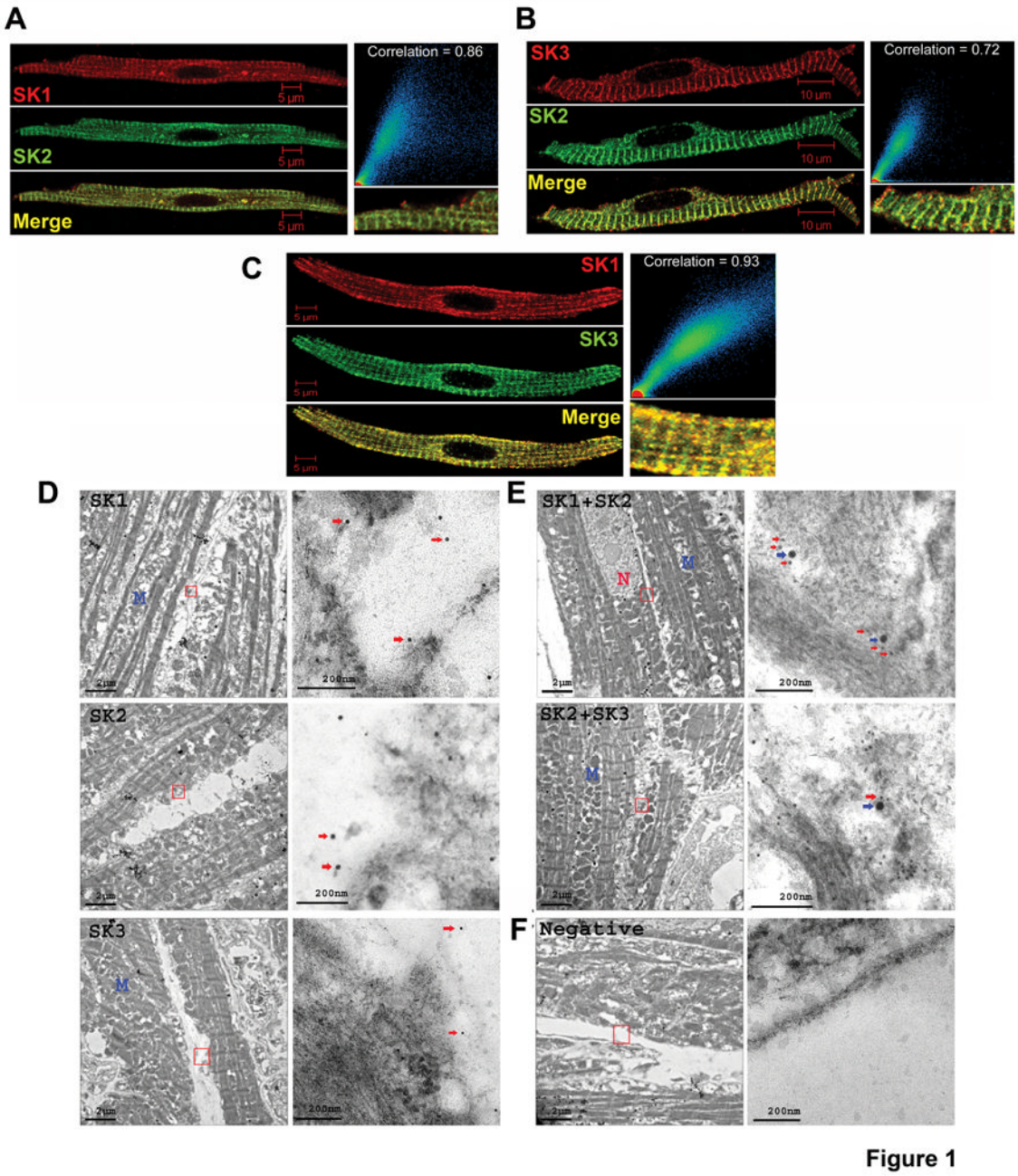

Figure 1. Subcellular distribution of SK1, SK2, and SK3 channel subunits in isolated mouse atrial myocytes using immunohistochemistry and immune-EM

Confocal photomicrographs of single isolated mouse atrial myocytes doubly stained with anti-SK antibodies in different combinations as follows: (A) goat anti-SK1 and rabbit anti-SK2, (B) rabbit anti-SK2 and goat anti-SK3, and (C) rabbit anti-SK1 and mouse anti-SK3 antibodies. Scale bars are 5 μm except in panel B (10 μm). Merged images are shown in third row of each panel. Scatter plots in the right panels show high correlation between different SK channel subunits. All pixels in the images have been assigned a position on the Scatter plots and are placed according to the intensity of red or green color. In addition, merge images are shown at higher magnification in the right panels. D-E, Electron

photomicrographs showing the ultra-structure of mouse atrial myocytes and subcellular distribution of SK1, SK2 and SK2 channel subunits. (D) Single immunolabeling for SK1, SK2 and SK3 channel subunits. Left, images taken under 3800× magnification with scale bars of 2 μm; Right, higher magnification images of areas marked by red boxes in the left panels with scale bars of 200 nm. Arrows indicate gold particles which are 10 nm, 15 nm and 5 nm for SK1, SK2 and SK3 staining, respectively. (E) Double labeling for SK1 and SK2, as well as SK2 and SK3 channel subunits. For SK1 and SK2 double labeling, 10 nm and 20 nm gold particle-conjugated secondary antibodies were used to localize SK1 and SK2 subunits, respectively. Note the clustering of SK1 (red arrows) and SK2 (blue arrows) channel subunits as shown by arrows. For SK2 and SK3, 20 nm and 10 nm gold-conjugated secondary antibodies were used to localize SK2 (blue arrows) and SK3 (red arrows) subunits, respectively. Note SK2 and SK3 channels are closely located as shown by arrows. (F) Negative controls are labeled by gold-conjugated secondary antibodies only and are devoid of any gold particles. N, nucleus; M, mitochondria.

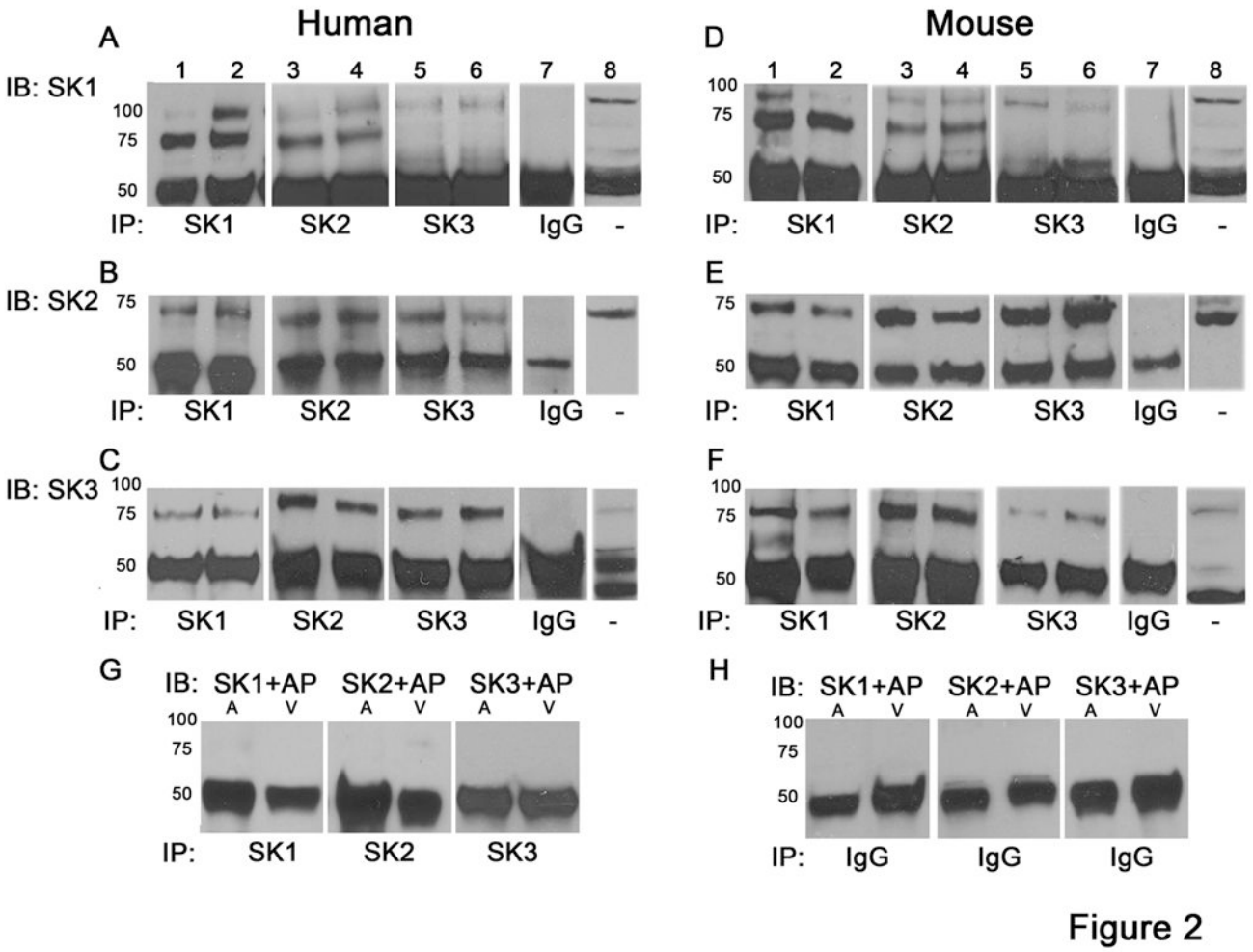

Figure 2. Heteromultimeric protein complexes of SK1, SK2, and SK3 channels detected from atrial and ventricular tissues using co-IP

Human (A-C) and mouse (D-F) atrial (Lanes 1, 3, 5) and ventricular (Lanes 2, 4, 6) tissue homogenates were immunoprecipitated (IP) with anti-SK antibodies, proteins were eluted and Western blot analysis (IB) was performed. The experiments were repeated a total of 6 times. (A,D) Immunoprecipitation of SK1 channel protein by anti-SK2 as well as anti-SK3 antibodies coupled to agarose beads, represented by a 70 kD band in the immunoblot. Both monomers and dimers were detected as distinct bands. (B,E) Immunoprecipitation of SK2 channel protein by anti-SK1 as well as anti-SK3 antibodies coupled to agarose beads, represented by a 70 kD band in the immunoblot. (C,F) Immunoprecipitation of SK3 channel protein by anti-SK2 as well as anti-SK3 antibodies coupled to agarose beads, represented by >70 kD band in the immunoblot. Negative control was performed by immunoblotting of eluted proteins immunoprecipitated with non-specific IgG (Lane 7, A-F) while positive control was performed using tissue homogenates (Lane 8, A-F). Lane 7 & 8 contained mixture of atrial and ventricular homogenates. (G) Control experiments were performed using mouse atrial (A) and ventricular (V) tissue homogenates immunoprecipitated (IP) with anti-SK antibodies, proteins were eluted and Western blot analysis (IB) was performed using anti-SK antibodies pre-incubated with their corresponding antigenic peptide (AP) in a ratio of 1:5. (H). Additional control experiments were performed using mouse atrial (A) and ventricular (V) tissue homogenates immunoprecipitated (IP) with non-specific normal rabbit

anti-IgG antibodies, proteins were eluted and Western blot analysis (IB) was performed with anti-SK antibodies. In both G & H, except for heavy chain band of 50 kD, no other bands were detected.

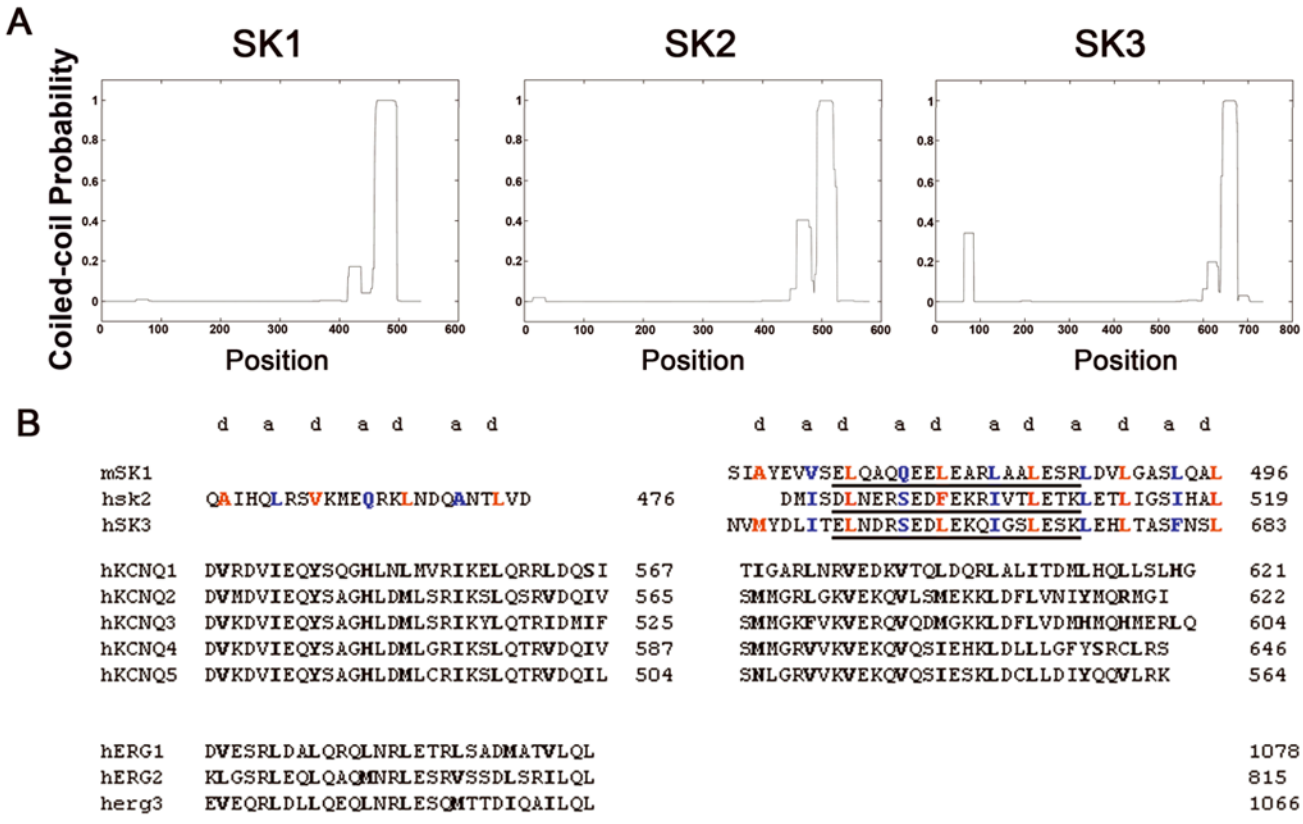

Figure 3

Figure 3. Tetramerizing Coiled-coil domains (CCDs) in SK1, 2 and 3 channels

(A) Coiled-coil probability for cardiac SK channel proteins using COILS with scanning window of 21. (B) Amino acid sequence alignment of C-termini from mammalian SK1, SK2, SK3, KCNQ (K_V7) and hERG ($K_V11.1$) channels demonstrating the presence of bimodular TCC domains. “a” and “d” coiled-coil positions are indicated and color coded as blue and red, respectively in second CCD of SK2 channel protein. Underlined amino acid residues in SK1, SK2, and SK3 sequence denote the synthesized inhibitory peptides used in electrophysiological studies. m: mouse, h: human.

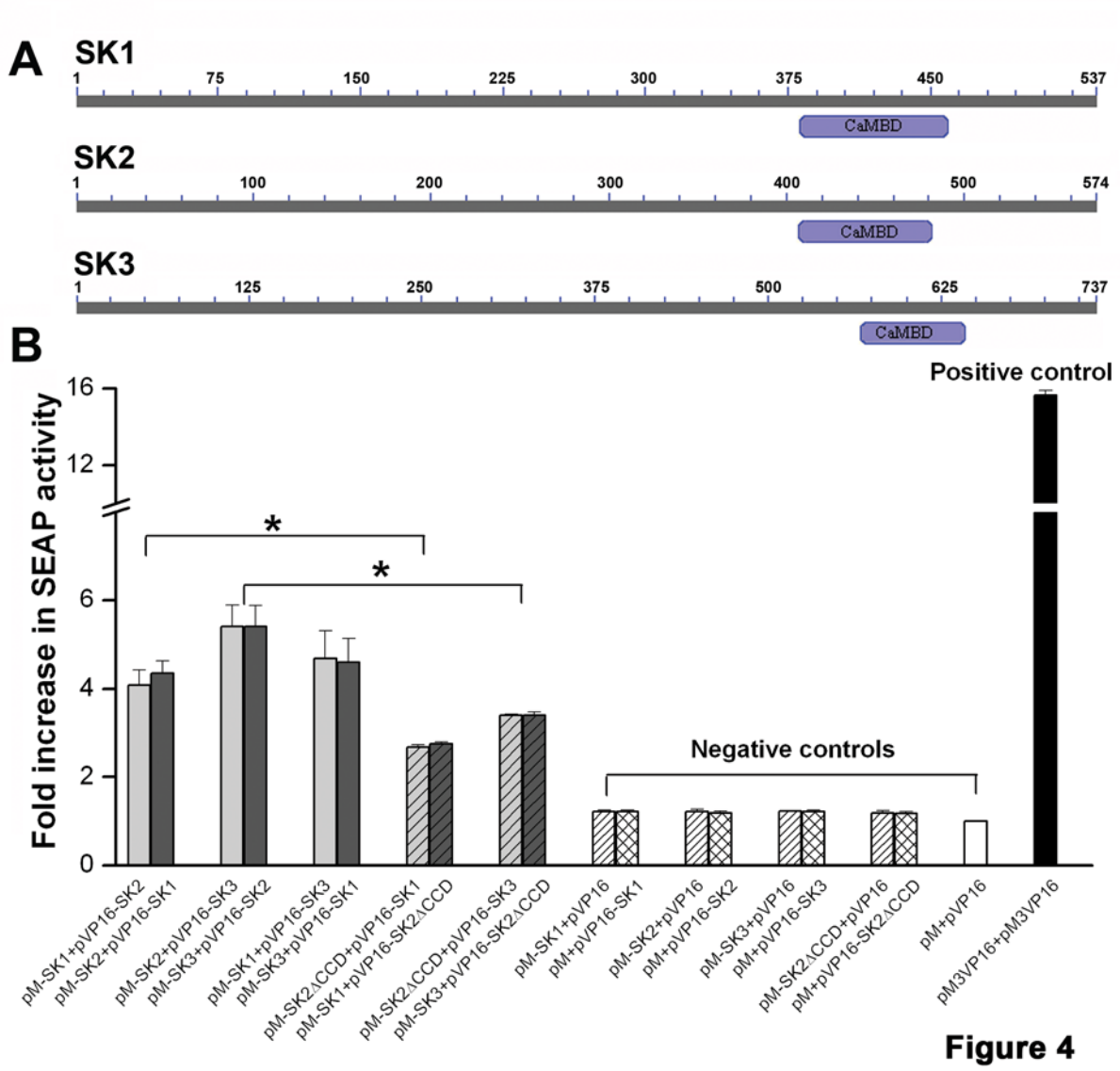

Figure 4. Identification of interaction between different SK channel subunits using*in vitro*interaction assay

Protein-protein interactions were assayed using the c-terminal fusion constructs of SK1-3 in pM and pVP16 vectors. (A) Schematic diagrams of cardiac SK1-SK3 proteins depicting the location of CaMBD. CaMBD and the region toward the C-terminus were used for the construction of the fusion proteins. (B) Protein-protein interactions among SK1, 2 and 3 C-termini are depicted by the fold increase of SEAP activity over controls. The roles of CCDs in SK2 channel in the interaction between different SK channel subunits were directly tested using SK2 C terminal constructs with deletion of the CCD domains (pM-SK2-ΔCCD and pVP16-SK2-ΔCCD).

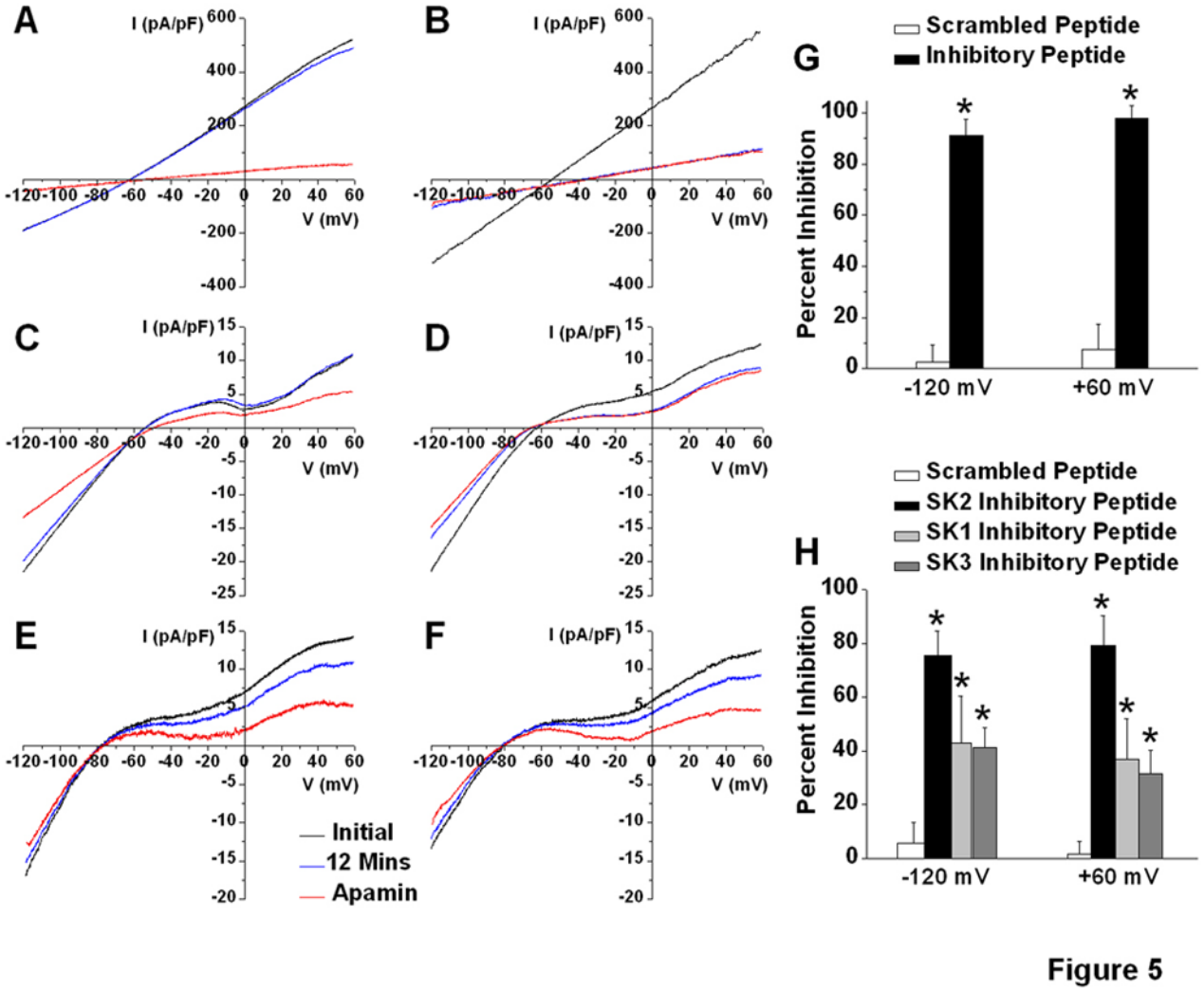

Figure 5

Figure 5. Peptides derived from the SK1, SK2 and SK3 CCD inhibit $I_{K,Ca}$ in atrial myocytes

A voltage-ramp protocol was applied from -120 to +60 mV at a holding potential of -55 mV. $I_{K,Ca}$ was recorded immediately after establishment of whole-cell mode (black line), 12 minutes thereafter (blue line) and after application of apamin (100 pM, red line). (A&B) $I_{K,Ca}$ density (pA/pF) recorded from tsA201 cells expressing SK2 current using scrambled (A) compared to SK2 (B) inhibitory peptides, respectively. (C-D) $I_{K,Ca}$ density recorded from mouse atrial myocytes using scrambled (C) compared to SK2 (D), SK1 (E), or SK3 (F) inhibitory peptides, respectively. (G&H) Summary data of percent inhibition of apamin-sensitive $I_{K,Ca}$ at -120 and +60 mV from tsA201 cells (G) and atrial myocytes (H), respectively (n=4-6), *p<0.05 comparing the inhibitory peptides to scrambled peptide.